**Serb. Astron. J. (2026), OnLine-First**
**DOI:** https://doi.org/10.2298/SAJ250505001S

**UDC 523.9 : 523.31 : 519.25**
Original scientific paper

# THE ATMOSPHERE OF SUPERGIANT STAR HD 7927 (F0 Ia): FUNDAMENTAL PARAMETERS AND CHEMICAL COMPOSITION

**Z. A. Samedov**[12] and **G. M. Hajiyeva**[23]

[1] *Department of Astrophysics, Baku State University, Z. Khalilov str.23, AZ 1148, Baku, Azerbaijan*

[2] *Division of Physics of stellar atmospheres and magnetism, Shamakhy Astrophysical Observatory, Shamakhy, AZ 5600 Azerbaijan*

E–mail: *haciyevagunay@yahoo.com*

[3] *Graduate School of Science, Art and Technology, Khazar University, 41 Mahsati Str., AZ 1096, Baku, Azerbaijan*

(Received: May 5, 2025; Accepted: November 17, 2025)

**SUMMARY: The atmosphere of supergiant star HD 7927 (F0 Ia) is investigated by the method of atmospheric model. The effective temperature and surface gravity are determined by comparing the observed and theoretical values of photometrical indices $[c_1]$, $Q$, and equivalent widths of Balmer lines: $T_{\rm eff} = 7350 \pm 200$ K, $\log g = 0.4 \pm 0.2$. The microturbulence parameter is evaluated as $\xi_t = 7.5 \pm 1$ km/s, based on studies of Fe II lines. The chemical composition of the star is determined. In the atmosphere of HD 7927, the C turned out to be a deficit, N, and Na in excess, the other investigated elements practically display solar abundance.**

**Key words. Stars: supergiants – Stars: atmospheres – Stars: abundances**

## 1. INTRODUCTION

The chemical composition of A, F, and G class supergiants has garnered significant attention in recent decades. According to the theory of chemical evolution, the abundances of light elements in the atmospheres of A-, F-, and G-type supergiant stars change over the course of stellar evolution, and the observed abundances differ from those present in the primordial material from which these stars originally formed (e.g., Ekström et al. 2012). Specifically, a deficit of carbon (C) and abundance of nitrogen (N) are expected to be observed in the atmospheres of supergiants belonging to spectral classes A, F, and G.

The study of chemical composition of A, F, and G supergiants, along with the comparison of the obtained data with predictions of chemical evolution theory, remains a topical issue in astrophysics.

Boyarchuk and Lyubimkov (1983) have observed that, in addition to the deviations in abundances of carbon (C) and nitrogen (N) in the atmospheres of A, F, and G class supergiants, there is also an overabundance of sodium (Na). They hypothesized that this excess sodium can be explained by conversion of a certain amount of neon (Ne) into sodium through the cyclic Ne − Na reactions. This excess sodium is expected to be released into the atmosphere as a result of deep mixing processes.

In our previous paper (Samedov and Hajieva 2024), we studied the atmosphere of the hypergiant star $\rho$ Cas (HR 9045, HD 224014). In the present work, we have determined the chemical composition of the F spectral class supergiant HD 7927 (F0 Ia). The star HD 7927 (F0 Ia) is one of the brightest stars in our Galaxy: Mv $= -9\overset{\rm m}{.}16$ (Kovtyukh et al. 2012).

Due to its high luminosity, this star may be approaching the hypergiant stage, which is a very rare type of star, with only a few examples identified in our Galaxy. This makes the object particularly intriguing and valuable for further investigation.

## 2. OBSERVATIONAL MATERIAL

The spectra of HD 7927 (F0 Ia) star were obtained on December 15, 2018, using the spectrograph with a CCD matrix of the 2-meter telescope of the Shamakhy Astrophysical Observatory of the Republic of Azerbaijan (R=56000, S/N=150-400). The analysis was conducted over the wavelength interval 3900–7800 Å. The analysis of spectrograms, were conducted using the DECH package programs, which were specifically developed by Galazutdinov (1992). We have assessed the equivalent widths of the spectral lines using two distinct methods: direct integration and Gaussian approximation. The direct integration method involves calculating the equivalent width by numerically integrating the area under the absorption or emission line profile, which provides a precise measurement of the line. In contrast, the Gaussian approximation method simplifies the line profile by assuming it follows a Gaussian distribution, allowing for estimation of the equivalent width based on the width and amplitude of a fitted Gaussian curve.

The equivalent widths of the Balmer hydrogen lines were measured as follows: $W(H_\beta) = 4.41$ Å, $W(H_\gamma) = 4.02$ Å, and $W(H_\delta) = 3.91$ Å. The equivalent widths of the spectral lines used in this study are provided in Tables 1 and 2.

The measurement error for the equivalent widths ($W_\lambda$) has been carefully controlled and it does not exceed 5%, ensuring high accuracy and reliability of our data.

## 3. PARAMETERS OF ATMOSPHERE: EFFECTIVE TEMPERATURE AND SURFACE GRAVITY

The atmosphere of the HD 7927 star was studied by the model method. This method has been extensively described (Lyubimkov et al. 2010). We have determined the effective temperature ($T_{\rm eff}$) and surface gravity ($\log g$) of the star HD 7927 based on the following criteria:

1. A comparison of the observed and theoretically calculated equivalent widths was carried out using the $H_\beta, H_\gamma$, and $H_\delta$ spectral lines of the Balmer series.

2. Comparison of observed and theoretically calculated values for index $[c_1]$.

3. Comparison of observed and theoretically calculated values for index Q.

In the narrowband four-color Strömgren photometric system (uvby) and the broadband Johnson photometric system (UBV), the indices $[c_1]$ and Q are defined by formulas $[c_1] = c_1 - 0.2(b-y)$ and Q = (U-B)-0.72(B-V), respectively. The indices $[c_1]$ and Q are free from effects of interstellar extinction.

By comparing the experimental values of the above-mentioned indices with their theoretical values, the parameters $\log g$ and $T_{\rm eff}$ were determined. The observed values of $[c_1]$ and Q were obtained from the catalog (Hauck and Mermilliod 1998). The calculations of color indices in the UBV and uvby systems, which are essential for determining Q and $[c_1]$, were carried out by Castelli and Kurucz (2003). The calculations of the equivalent widths of the Balmer lines were presented by Kurucz (1993).

Fig. 1 shows the diagram that determines $T_{\rm eff}$ and $\log g$ based on the above criteria. Based on Fig. 1 for parameters of the atmosphere of HD 7927 star, the following values are taken: $T_{\rm eff} = 7350 \pm 200$ K, $\log g = 0.4 \pm 0.2$.

The fundamental parameters of HD 7927 have been determined by several authors. Rosenzweig and Anderson (1993) constructed a non-LTE atmospheric model and determined $T_{\rm eff} = 7200 \pm 100$ K and $\log g = 0.4 \pm 0.1$ by comparing the theoretical and observed energy distributions in the UV and visible regions of the spectrum, as well as the theoretical and observed profiles of the H$\delta$, Ca II(H and K), and Mg II lines.

The effective temperature was determined as $T_{\rm eff} = 7300$ K from the UBVRI and uvby photometry in Arellano Ferro et al. (1988). By adopting $M_V = -8\overset{m}{.}4$ and $T_{\rm eff} = 7300$ K, the authors calculated the radius of the star $R = 245\,R_\odot$ based on evolutionary tracks, as well as the stellar mass $M = 17\,M_\odot$, and surface gravity $\log g = 0.9$ (Iben 1967). In Kovtyukh et al. (2012) and Luck (2014), the effective temperature was determined using the ratio of central intensities of selected line pairs, yielding $T_{\rm eff} = 7340$ K and $T_{\rm eff} = 7160$ K, respectively. Surface gravity values of $\log g = 1.0$ and $\log g = 2.0$ were also derived in Kovtyukh et al. (2012) and Luck (2014), respectively, based on ionization equilibrium.

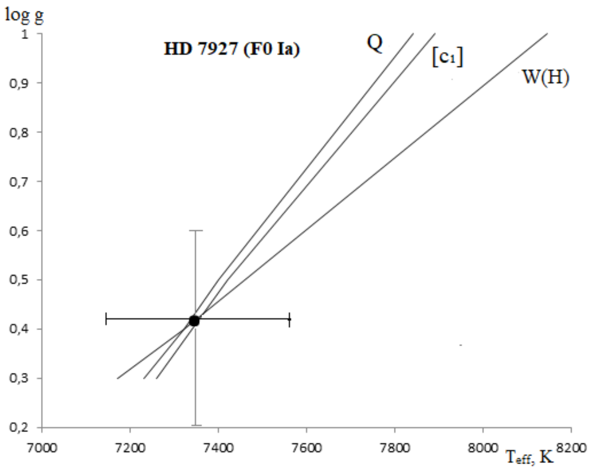


**Fig. 1**: $T_{\rm eff} - \log g$ diagram. The lines are constructed based on a comparison between observed and theoretical values of the equivalent widths of the $H_\beta, H\gamma$, and $H_\delta$ lines, as well the $[c_1]$ and Q indices. The filled circle represents the accepted values of $T_{\rm eff}$ and $\log g$.

**Table 1**: List of used Fe II lines. For each line, the wavelength, excitation potentials of the lower energy levels, oscillator strengths, measured equivalent widths, and calculated iron abundances are shown.The mean value of the iron abundance is presented with the standard deviation.

| Line (λ Å) | $E_{excit}$ (eV) | log gf | W(mÅ) | log ε(Fe) | Line (λ Å) | $E_{excit}$ (eV) | log gf | W(mÅ) | log ε(Fe) |
|---|---|---|---|---|---|---|---|---|---|
| 4031.46 | 4.71 | -3.20 | 79 | 7.61 | 6147.73 | 3.87 | -2.73 | 281 | 7.63 |
| 4413.60 | 2.66 | -4.01 | 169 | 7.35 | 6149.24 | 3.87 | -2.73 | 279 | 7.62 |
| 4635.32 | 5.93 | -1.48 | 168 | 7.31 | 6238.38 | 3.87 | -2.64 | 267 | 7.38 |
| 4993.36 | 2.79 | -3.58 | 258 | 7.41 | 6239.95 | 3.87 | -3.44 | 138 | 7.52 |
| 5100.66 | 2.79 | -4.22 | 189 | 7.70 | 6369.46 | 2.88 | -4.29 | 127 | 7.53 |
| 5136.78 | 2.83 | -4.38 | 122 | 7.58 | 6416.92 | 3.87 | -2.75 | 246 | 7.38 |
| 5256.89 | 2.88 | -4.33 | 140 | 7.66 | 6432.65 | 2.88 | -3.75 | 229 | 7.48 |
| 5414.07 | 3.21 | -3.85 | 180 | 7.59 | 6446.43 | 6.20 | -2.02 | 51 | 7.35 |
| 5425.27 | 3.19 | -3.35 | 223 | 7.31 | 7449.34 | 3.87 | -3.30 | 138 | 7.41 |
| 5991.37 | 3.14 | -3.63 | 189 | 7.39 | 7515.88 | 3.89 | -3.42 | 78 | 7.27 |
| 6084.10 | 3.19 | -3.85 | 143 | 7.42 | 7711.71 | 3.89 | -2.54 | 269 | 7.32 |
| 6113.32 | 3.21 | -4.20 | 98 | 7.55 | | | | | |
| | | | | | | | | | $\log\varepsilon(\mathrm{Fe}) = 7.47 \pm 0.13$ |

It can be seen that the $T_{\rm eff}$ values reported in the literature are in good agreement with one another, and also with our results. However, there is a significant discrepancy in the reported values of log g. It should be noted that a value of log g = 2.0 is too high for a star of luminosity class Ia. In the determination of log g, the ionization equilibrium between Fe I and Fe II lines was used, and the calculations were carried out under the assumption of local thermodynamic equilibrium (LTE) (Kovtyukh et al. 2012, Luck 2014).

This led to an overestimation of log g, since deviations from LTE should have been taken into account in interpretation of Fe I line calculations. In Arellano Ferro et al. (1988), the calculation of log g is based on parameters $M_v$, R, and M whose accuracy is relatively low.

In Rosenzweig and Anderson (1993), log g was determined by comparing the observed and theoretically estimated values of certain spectral and photometric quantities. Theoretical values were derived from a non-LTE atmospheric model.

The value of log g determined by Rosenzweig and Anderson (1993) is in complete agreement with the value obtained in our study. This consistency reinforces confidence in the reliability of both our results and those presented by Rosenzweig and Anderson (1993). The method we used is thoroughly described in Lyubimkov et al. (2009), and its accuracy has been well validated.

## 4. MICROTURBULENT VELOCITY

Despite accounting for all known broadening mechanisms, it has not been possible to fully reproduce the observed profiles of spectral lines in stellar spectra. Consequently, it has been assumed that, in addition to the thermal motions of atoms, nonthermal motions also exist in stellar atmospheres. These motions are referred to as turbulent motions.

In astrophysics, turbulence is considered one of the key mechanisms responsible for spectral line broadening. The concept of turbulence was introduced to reconcile the discrepancies between observed and theoretically calculated spectral line profiles. Conventionally, two types of turbulence are distinguished: macroturbulence (large-scale) and microturbulence (small-scale).

Currently, the physical nature of both micro- and macroturbulence is under investigation. For example, in Asplund et al. (2000), three-dimensional radiative-hydrodynamical simulations of solar granulation were applied to formation of Fe I and Fe II lines. It was shown that the computed spectral line profiles closely match the observed ones, eliminating the need to introduce micro- or macroturbulence parameters. The classical concepts of micro- and macroturbulence are fully explained by the convective-granulation velocity fields, vibrational motions of the photosphere, and temperature inhomogeneities.

When studying stellar atmospheres using one-dimensional (1D) models, micro- and macroturbulent velocities are typically introduced to account for non-thermal broadening effects. In order to determine the microturbulent velocity ($\xi_t$), a set of spectral lines from a given atom or ion spanning a wide range of equivalent widths ($W_\lambda$) is required. The value of $\xi_t$ is then adjusted so that the derived elemental abundances remain independent of $W_\lambda$, ensuring that no artificial trend appears with increasing line strength.

The most numerous lines in the spectra of the studied stars were those of neutral iron (Fe I), followed by lines of ionized iron (Fe II). However, the lines of neutral iron can be subject to significant deviations from LTE.

If deviations from LTE are not taken into account, this will result in an underestimation of the determined iron content, log ε(Fe).

This was first demonstrated by Boyarchuk et al. for F-supergiants (Boyarchuk et al. 1985), and later confirmed by other authors for F- and G-stars (for example, Thévenin and Idiart 1999). Interestingly, in contrast to the Fe I lines, the Fe II lines were found to be insensitive to LTE effects. Therefore, in determining the microturbulent velocity in the stellar atmosphere, we used Fe II lines. In the determination of $\xi_t$, we consider only Fe II lines with equivalent

**Table 2**: List of lines.

| Line (λ, Å) | $E_{excit}$ (eV) | log gf | W (mÅ) | logε |
|---|---|---|---|---|
| **C I** | | | | |
| 4770.03 | 7.45 | -2.44 | 21 | 8.46 |
| 4932.65 | 7.65 | -1.66 | 58 | 8.30 |
| 5052.17 | 7.68 | -1.30 | 122 | 8.37 |
| 6014.84 | 8.64 | -1.58 | 13 | 8.24 |
| 6587.61 | 8.50 | -1.00 | 51 | 8.20 |
| 7087.83 | 8.64 | -1.44 | 14 | 8.13 |
| 7108.93 | 8.64 | -1.59 | 21 | 8.48 |
| 7111.47 | 8.64 | -1.08 | 55 | 8.43 |
| 7113.18 | 8.65 | -0.77 | 90 | 8.41 |
| 7115.17 | 8.64 | -0.93 | 78 | 8.48 |
| 7116.99 | 8.65 | -0.91 | 53 | 8.25 |
| 7476.18 | 8.77 | -1.57 | 16 | 8.45 |
| 7483.45 | 8.77 | -1.37 | 23 | 8.43 |
| | | | | logε(C) = 8.36±0.12 |
| **N I** | | | | |
| 7423.64 | 10.33 | -0.71 | 122 | 8.74 |
| 7442.30 | 10.33 | -0.38 | 189 | 8.82 |
| 7468.31 | 10.33 | -0.19 | 159 | 8.54 |
| | | | | logε(N) = 8.70±0.14 |
| **O I** | | | | |
| 6300.30 | 0.0 | -9.72 | 18 | 8.96 |
| | | | | logε(O) = 8.96 |
| **Na I** | | | | |
| 4668.56 | 2.10 | -1.31 | 13 | 6.67 |
| 5682.63 | 2.09 | -0.71 | 35 | 6.50 |
| 5688.21 | 2.10 | -0.45 | 84 | 6.87 |
| 6160.75 | 2.10 | -1.26 | 18 | 6.74 |
| | | | | logε(Na) = 6.70±0.15 |
| **Mg I** | | | | |
| 4057.51 | 4.33 | -1.20 | 97 | 7.63 |
| 4702.99 | 4.33 | -0.67 | 143 | 7.45 |
| 5528.41 | 4.33 | -0.62 | 172 | 7.42 |
| 5711.09 | 4.33 | -1.83 | 22 | 7.49 |
| | | | | logε(Mg) = 7.50±0.09 |
| **Si I** | | | | |
| 5690.43 | 4.91 | -1.77 | 15 | 7.53 |
| 7165.55 | 5.85 | -0.59 | 31 | 7.60 |
| 7409.08 | 5.59 | -0.62 | 21 | 7.41 |
| 7918.38 | 5.93 | -0.66 | 19 | 7.62 |
| | | | | logε(Si) = 7.54±0.09 |
| **Ca I** | | | | |
| 4425.44 | 1.87 | -0.45 | 41 | 6.08 |
| 4434.96 | 1.88 | -0.10 | 104 | 6.25 |
| 4435.68 | 1.88 | -0.57 | 37 | 6.16 |
| 4454.78 | 1.89 | 0.17 | 173 | 6.35 |
| 5512.99 | 2.92 | -0.26 | 20 | 6.31 |
| 5594.46 | 2.51 | 0.09 | 65 | 6.20 |
| 5857.45 | 2.92 | 0.33 | 40 | 6.10 |
| 6122.22 | 1.88 | -0.26 | 83 | 6.17 |
| 6162.17 | 1.89 | -0.04 | 120 | 6.19 |
| 6169.04 | 2.51 | -0.80 | 14 | 6.37 |
| 6169.57 | 2.51 | -0.53 | 15 | 6.15 |
| 6439.08 | 2.51 | 0.44 | 92 | 6.13 |
| | | | | logε(Ca) = 6.21±0.09 |
| **Sc II** | | | | |
| 4354.60 | 0.60 | -1.55 | 146 | 2.93 |
| 5239.82 | 1.45 | -0.74 | 202 | 2.98 |
| 5318.35 | 1.35 | -1.87 | 57 | 3.23 |
| 5641.00 | 1.49 | -0.99 | 168 | 3.08 |
| 5667.15 | 1.49 | -1.18 | 123 | 3.06 |
| 5669.03 | 1.49 | -1.07 | 147 | 3.06 |
| 6245.62 | 1.50 | -1.02 | 134 | 2.95 |
| 6320.85 | 1.49 | -1.82 | 45 | 3.14 |
| | | | | logε(Sc) = 3.05±0.10 |

Table 2: Continued.

| Line (λ, Å) | $E_{excit}$ (eV) | log gf | W (mÅ) | logε |
|---|---|---|---|---|
| **Ti II** | | | | |
| 4184.31 | 1.08 | -2.50 | 237 | 5.09 |
| 4316.79 | 2.04 | -1.61 | 276 | 5.17 |
| 4411.06 | 3.08 | -0.57 | 280 | 4.98 |
| 4421.94 | 2.05 | -1.38 | 240 | 4.73 |
| 4544.02 | 1.24 | -2.49 | 159 | 4.77 |
| 4545.14 | 1.13 | -2.80 | 176 | 5.06 |
| 4708.66 | 1.23 | -2.40 | 234 | 5.02 |
| 4798.53 | 1.08 | -2.68 | 175 | 4.88 |
| 5010.21 | 3.08 | -1.33 | 127 | 4.88 |
| 5013.69 | 1.57 | -2.01 | 243 | 4.90 |
| 5069.09 | 3.11 | -1.41 | 128 | 5.00 |
| 5381.02 | 1.56 | -1.96 | 242 | 4.81 |
| | | | | logε(Ti) = 4.94±0.13 |
| **V II** | | | | |
| 4035.63 | 1.79 | -0.68 | 266 | 3.96 |
| 4036.76 | 1.97 | -1.67 | 93 | 4.01 |
| 4039.57 | 1.81 | -1.73 | 31 | 3.72 |
| 5303.25 | 2.27 | -2.05 | 20 | 3.91 |
| | | | | logε(V) = 3.90±0.13 |
| **Cr II** | | | | |
| 4145.78 | 5.30 | -1.20 | 140 | 5.72 |
| 4252.63 | 3.84 | -2.05 | 194 | 5.33 |
| 4812.35 | 3.85 | -2.03 | 183 | 5.61 |
| 4836.23 | 3.84 | -1.96 | 210 | 5.69 |
| 4884.60 | 3.85 | -2.16 | 178 | 5.71 |
| 5279.86 | 4.06 | -1.93 | 231 | 5.79 |
| 5305.86 | 3.81 | -2.30 | 184 | 5.73 |
| 5313.58 | 4.06 | -1.50 | 220 | 5.40 |
| 5334.87 | 4.05 | -1.59 | 230 | 5.53 |
| 5478.37 | 4.16 | -1.90 | 166 | 5.62 |
| 5502.08 | 4.15 | -2.04 | 133 | 5.58 |
| 5503.22 | 4.13 | -2.29 | 104 | 5.68 |
| 6053.47 | 4.72 | -2.20 | 33 | 5.56 |
| | | | | logε(Cr) = 5.61±0.13 |
| **Y II** | | | | |
| 4398.01 | 0.13 | -0.90 | 240 | 2.31 |
| 4900.12 | 1.03 | 0.10 | 286 | 2.20 |
| 5205.72 | 1.03 | -0.19 | 274 | 2.39 |
| 5402.78 | 1.83 | -0.36 | 70 | 2.18 |
| 5544.61 | 1.73 | -0.83 | 43 | 2.30 |
| | | | | logε(Y) = 2.28±0.09 |
| **Zr II** | | | | |
| 4077.04 | 0.96 | -1.69 | 14 | 2.56 |
| 4149.20 | 0.80 | -0.04 | 278 | 2.61 |
| 4211.88 | 0.52 | -1.04 | 132 | 2.62 |
| 4359.72 | 1.23 | -0.51 | 131 | 2.64 |
| 4496.96 | 0.71 | -0.89 | 160 | 2.72 |
| | | | | logε(Zr) = 2.63±0.06 |
| **Ba II** | | | | |
| 5853.68 | 0.60 | -1.00 | 93 | 2.26 |
| 6141.71 | 0.70 | -0.08 | 287 | 2.32 |
| 6496.90 | 0.60 | -0.38 | 258 | 2.38 |
| | | | | logε(Ba) = 2.32±0.06 |
| **La II** | | | | |
| 4086.71 | 0.00 | -0.15 | 54 | 1.07 |
| 4429.72 | 0.23 | -0.49 | 26 | 1.18 |
| 4748.73 | 0.92 | -0.54 | 10 | 1.03 |
| | | | | logε(La) = 1.09±0.08 |

Table 2: Continued.

| **Line (λ, Å)** | **$E_{excit}$ (eV)** | **log gf** | **W (mÅ)** | **log$\varepsilon$** |
|---|---|---|---|---|
| **Ce II** | | | | |
| 4042.58 | 0.49 | 0.18 | 30 | 1.57 |
| 4222.59 | 0.12 | -0.30 | 20 | 1.53 |
| 4364.65 | 0.49 | -0.23 | 10 | 1.42 |
| 4449.33 | 0.61 | 0.04 | 20 | 1.56 |
| 4486.91 | 0.29 | -0.47 | 13 | 1.61 |
| 5393.39 | 0.62 | -0.06 | 13 | 1.40 |
| | | | | log$\varepsilon$(Ce) = 1.52±0.08 |
| **Nd II** | | | | |
| 4069.27 | 0.06 | -0.57 | 13 | 1.43 |
| 4156.08 | 0.18 | 0.20 | 72 | 1.58 |
| 4358.17 | 0.32 | -0.28 | 11 | 1.22 |
| 5092.79 | 0.38 | -0.70 | 6 | 1.35 |
| | | | | log$\varepsilon$(Nd) = 1.40±0.15 |
| **Gd II** | | | | |
| 4251.74 | 0.38 | -0.37 | 15 | 1.09 |
| 4280.53 | 0.35 | -0.67 | 8 | 1.07 |
| | | | | log$\varepsilon$(Gd) = 1.08±0.01 |

widths W $< 280\,m$Å. These lines are formed in deeper layers of the atmosphere, where they can be considered to be in a planeparallel configuration in LTE.

Based on the determined parameters $T_{\rm eff}$ and $\log g$, we calculated the corresponding model atmosphere using Kurucz's ATLAS 9 program (Kurucz 1993). Employing the model obtained, we calculated the iron abundance $\log \varepsilon$(Fe II) for several values of $\xi_t$. The iron abundance derived from the selected Fe II spectral lines at $\xi_t = 7.5 \pm 1$ km/s is presented in Table 1.

The iron abundance was determined by comparing the calculated and observed equivalent widths of Fe II spectral lines.

We used atomic data for spectral lines from the VALD-3 database (Ryabchikova et al. 2015).

The determination of the microturbulent velocity parameter ($\xi_t$) for the HD 7927 star is illustrated in Fig. 2.

As can be seen from Fig. 2, there is no correlation between $\log \varepsilon$ and $W\lambda$ at $\xi_t = 7.5$ km/s.

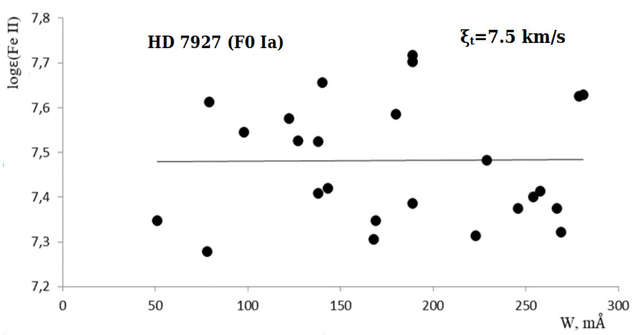


**Fig. 2**: Determination of microturbulent velocity. The straight line indicates when $\xi_t = 7.5$ km/s, there is no correlation between the iron abundance, $\log \varepsilon$(Fe II), and the equivalent widths of the spectral lines ($W_\lambda$).

## 5. ABUNDANCE OF ELEMENTS

When analyzing microturbulence ($\xi_t$), the iron content is simultaneously determined from the Fe II lines: $\log \varepsilon(\mathrm{Fe}) = 7.47$. Note that the abundances of elements are given on a logarithmic scale.

$$\lg \varepsilon(el) = \lg \frac{N(el)}{N(H)} + 12$$

For hydrogen, it is assumed that $\log \varepsilon(\mathrm{H}) = 12$. Applying our model (the basic parameters: $T_{\rm eff} = 7350 \pm 200$ K, $\log\ g = 0.4 \pm 0.2$) we calculated the abundance of the elements at $\xi_t = 7.5 \pm 1$ km/s. We present the results in Tables 1 and 2. The difference in the abundances of elements $\Delta \log \varepsilon = \lg \varepsilon_*(el) - \lg \varepsilon_\odot(el)$ in the star and Sun is presented in Table 3, and Fig. 3. Solar abundances $\log \varepsilon_\odot$(el) are taken from Scott et al. (2015) and Grevesse et al. (2015).

**Table 3**: The difference in elemental abundances between HD 7927 and the Sun.

| **Element** | **log $\varepsilon$** | **log $\varepsilon_\odot$** | **$\Delta$log $\varepsilon$ =log $\varepsilon$−log $\varepsilon_\odot$** |
|---|---|---|---|
| C | 8.36 | 8.43 | -0.07 |
| N | 8.70 | 7.83 | 0.87 |
| O | 8.96 | 8.69 | 0.27 |
| Na | 6.70 | 6.21 | 0.49 |
| Mg | 7.50 | 7.59 | -0.09 |
| Si | 7.54 | 7.51 | 0.03 |
| Ca | 6.21 | 6.32 | -0.11 |
| Sc | 3.05 | 3.16 | -0.11 |
| Ti | 4.94 | 4.93 | 0.01 |
| V | 3.90 | 3.89 | 0.01 |
| Cr | 5.61 | 5.62 | -0.01 |
| Fe | 7.47 | 7.47 | 0.00 |
| Y | 2.28 | 2.21 | 0.07 |
| Zr | 2.63 | 2.59 | 0.04 |
| Ba | 2.32 | 2.25 | 0.07 |
| La | 1.09 | 1.11 | -0.02 |
| Ce | 1.52 | 1.58 | -0.06 |
| Nd | 1.40 | 1.42 | -0.02 |
| Gd | 1.08 | 1.08 | 0.00 |

Colored circles represent the elements (C, N, Na) for which literature data indicate that non-LTE corrections are required. The arrows indicate that these corrections tend to decrease the derived abundances. According to references (Lyubimkov et al. 2011, 2015, 2019), the N I and C I lines are affected by non-LTE effects. Therefore, corrections of approximately $-(0.5-0.6)$ dex should be applied to $\log \varepsilon$(N), and $-(0.2-0.3)$ dex to $\log \varepsilon$(C), the non-LTE effect on the oxygen abundance derived from the O I 6300.30$\mathring{A}$ line is found to be insignificant. According to the study by Andrievsky et al. (2002), the influence of non-LTE corrections on the sodium abundance, expressed as log$\varepsilon$(Na), is estimated to be within the range of (0.1-0.2) dex.The mean values of the elements are presented with their standard deviations.

In the spectrum of HD 7927, both neutral and ionized lines of iron-group elements were observed. The abundances of iron-group elements were determined from the ionized lines. The deviation from LTE has a

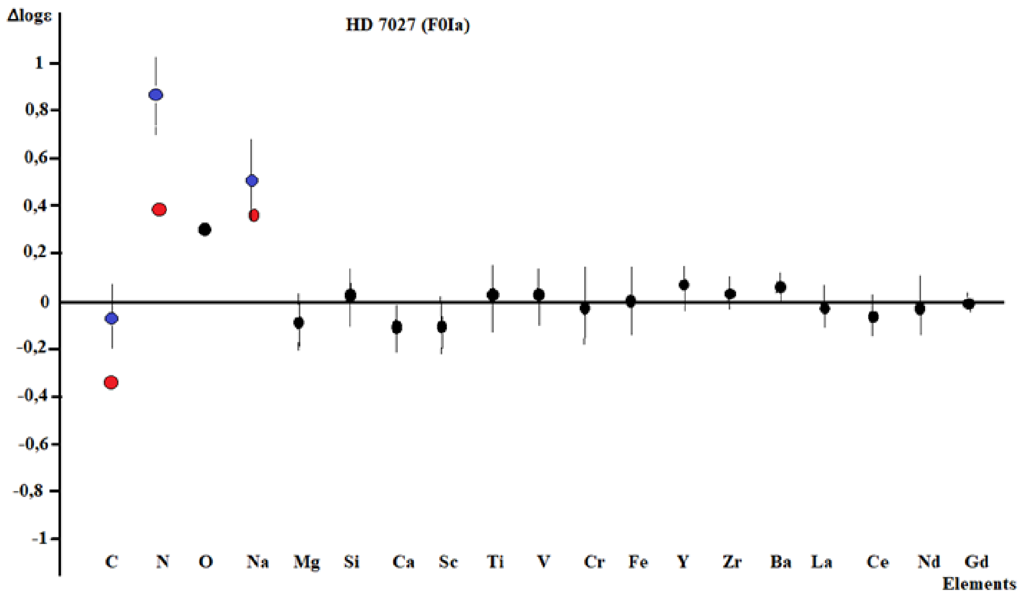


**Fig. 3**: The difference in abundances of elements between HD 7927 and the Sun. The horizontal line at zero represents the solar abundances. Elements corrected for the non-LTE effects are shown with blue circles, and these corrections are indicated with red circles.

weaker effect on the lines of ionized atoms compared to its effect on the lines of neutral atoms.

As can be seen from Fig. 3, in the atmosphere of HD 7927, carbon shows a deficiency, while nitrogen (N) and sodium (Na) are in excess. The other investigated elements exhibit nearly solar abundances.

This suggests that the star HD 7927 was formed from matter with a chemical composition similar to that of the Sun. The oxygen content and metallicity have remained unchanged, while evolutionary changes have been observed in compositions of carbon (C), nitrogen (N), and sodium (Na). This conclusion is of particular interest in the context of galactic chemical evolution models.

The total abundance of the C, N, and O elements, i.e., $\log\varepsilon(\mathrm{C+N+O})$, is equal to 9.07 after applying the non-LTE corrections to $\log\varepsilon(\mathrm{C})$ and $\log\varepsilon(\mathrm{N})$. It should be noted that $\log\varepsilon(\mathrm{O})$ was derived based on a single spectral line, and therefore may not be considered reliable. It is likely that the slightly higher value of $\log\varepsilon(\mathrm{C+N+O})$ in the atmosphere of HD 7927, compared to that of the Sun (8.92), is due to this uncertainty.

The elemental abundances in the atmospheres of giants and supergiants have been determined by numerous authors (for example Lyubimkov et al. 2009, Lyubimkov et al. 2010, Lyubimkov et al. 2011, Lyubimkov et al. 2015, Lyubimkov et al. 2019, Luck et al. 2006), and it has been shown that the oxygen content and metallicity of these stars are similar to those of the Sun, with carbon in deficit, and nitrogen and sodium in excess.

## 6. CONCLUSION

The main results obtained in this study are summarized below.

1. The effective temperature and surface gravity of the HD 7927 star were determined using the atmospheric model method. The following values for the effective temperature and surface gravity were found: $T_{\mathrm{eff}} = 7350 \pm 200$ K, $\log\ g = 0.4 \pm 0.1$.

2. The microturbulence parameter was determined to be $\xi_t = 7.5 \pm 1$ km/s based on the study of Fe II lines.

3. The elemental abundances in the atmosphere of HD 7927 were determined and compared with those of the Sun. A deficiency of carbon (C), and an excess of nitrogen (N) and sodium (Na) were found. The abundances of other studied elements are close to solar values. This suggests that HD 7927 was formed from matter with a chemical composition similar to that of the Sun. The oxygen content and metallicity have remained unchanged, while evolutionary changes have been observed in the composition of carbon (C), nitrogen (N), and sodium (Na). Thus, the predictions of evolutionary theory are confirmed by these observations.

## REFERENCES

Andrievsky, S. M., Egorova, I. A., Korotin, S. A. and Burnage, R. 2002, A&A, 389, 519

Arellano Ferro, A., Parrao, L. and Giridhar, S. 1988, PASP, 100, 993

Asplund, M., Nordlund, Å., Trampedach, R., Allende Prieto, C. and Stein, R. F. 2000, A&A, 359, 729

Boyarchuk, A. A. and Lyubimkov, L. S. 1983, Bulletin Crimean Astrophysical Observatory, 66, 119
Boyarchuk, A. A., Lyubimkov, L. S. and Sakhibullin, N. A. 1985, Ap, 22, 203
Castelli, F. and Kurucz, R. L. 2003, in IAU Symposium, Vol. 210, Modelling of Stellar Atmospheres, ed. N. Piskunov, W. W. Weiss and D. F. Gray, A20
Ekström, S., Georgy, C., Eggenberger, P., et al. 2012, A&A, 537, A146
Galazutdinov, G. 1992, Preprint SAO RAS, No. 92
Grevesse, N., Scott, P., Asplund, M. and Sauval, A. J. 2015, A&A, 573, A27
Hauck, B. and Mermilliod, M. 1998, A&AS, 129, 431
Iben, Jr., I. 1967, ARA&A, 5, 571
Kovtyukh, V. V., Gorlova, N. I. and Belik, S. I. 2012, MNRAS, 423, 3268
Kurucz, R. 1993, Robert Kurucz CD-ROM, 13
Luck, R. E. 2014, AJ, 147, 137
Luck, R. E., Kovtyukh, V. V. and Andrievsky, S. M. 2006, AJ, 132, 902
Lyubimkov, L. S., Rachkovskaya, T. M. and Poklad, D. B. 2009, Ap, 52, 217
Lyubimkov, L. S., Lambert, D. L., Rostopchin, S. I., Rachkovskaya, T. M. and Poklad, D. B. 2010, MNRAS, 402, 1369
Lyubimkov, L. S., Lambert, D. L., Korotin, S. A., et al. 2011, MNRAS, 410, 1774
Lyubimkov, L. S., Lambert, D. L., Korotin, S. A., Rachkovskaya, T. M. and Poklad, D. B. 2015, MNRAS, 446, 3447
Lyubimkov, L. S., Korotin, S. A. and Lambert, D. L. 2019, MNRAS, 489, 1533
Rosenzweig, P. and Anderson, L. 1993, ApJ, 411, 207
Ryabchikova, T., Piskunov, N., Kurucz, R. L., et al. 2015, PhyS, 90, 054005
Samedov, Z. A. and Hajieva, G. M. 2024, SerAJ, 209, 33
Scott, P., Asplund, M., Grevesse, N., Bergemann, M. and Sauval, A. J. 2015, A&A, 573, A26
Thévenin, F. and Idiart, T. P. 1999, ApJ, 521, 753

# АТМОСФЕРА ЗВЕЗДЕ СУПЕРЏИНА HD 7927 (F0 Ia): ФУНДАМЕНТАЛНИ ПАРАМЕТРИ И ХЕМИЈСКА ЗАСТУПЉЕНОСТ

**Z. A. Samedov**[1,2] **and G. M. Hajiyeva**[2,3]

[1]*Department of Astrophysics, Baku State University, Z. Khalilov str.23, AZ 1148, Baku, Azerbaijan*

[2]*Division of Physics of stellar atmospheres and magnetism, Shamakhy Astrophysical Observatory, Shamakhy, AZ 5600 Azerbaijan*

E–mail: *haciyevagunay@yahoo.com*

[3]*Graduate School of Science, Art and Technology, Khazar University, 41 Mahsati Str., AZ 1096, Baku, Azerbaijan*

УДК 523.9 : 523.31 : 519.25
*Оригинални научни рад*

Методом моделирања атмосфере изучена је атмосфера звезде суперџина HD 7927 (F0 Ia). Поређењем посматраних и теоријских вредности фотометријских индекса $[c_1]$, $Q$ и еквивалентне ширине Балмерових линија одређене су ефективна температура и површинска гравитација које износе $T_{\rm eff} = 7350 \pm 200\,{\rm K}$ и $\log g = 0.4 \pm 0.2$, редом. На основу анализе Fe II линија процењена је вредност микротурбуленција од $\xi_t = 7.5 \pm 1\,{\rm km\,s^{-1}}$. Одређена је хемијска заступљеност у атмосфери HD 7927; уочен је недостатак угљеника, вишак азота и натријума, док је заступљеност осталих елемената слична Сунчевој заступљености.